Problem Chosen	2022 ShuWei Cup Summary Sheet	Team Control Number
D		2022092812658

Triple La Niña Warns People to Protect the Environment！

Summary

Hidden in the equatorial Middle East Pacific is a "little girl" who may appear when sea surface temperatures continue to be unusually cold over a wide range of areas. Her name is "La Niña". The advent of this extreme climate has had a serious impact on many cities in southern China. Several days of hot weather and rare drought have left southern cities vulnerable to La Niña.

For problem 1, statistical analysis of major countries and regions where extreme weather events occur and prediction of future occurrences are conducted. First, this paper **quantifies Extreme Climate Events** and **establishes TLNI index** to represent them. Then, the **Extreme Climate Impact Model (ECIM)** is constructed by using the **Greenhouse Gas Concentration**, **Sea Level Index**, **Glacier Retraction Index** and other indicators to comprehensively analyze the countries and regions where extreme climate occurs. The **Chi-square Coefficient** and **Pearson correlation coefficient** are used to test the above indexes. The **Probability of Extreme Climate Events** are then quantified and measured by the **TLNPI index**. This paper establishes an **Extreme Climate Prediction Model based on Two-layer Hopfield Neural Network (ECPM-THNN)**, uses TLNPI index as the energy function of the network and trains the network. As a result, countries in the central and Eastern Pacific have a **4.71% chance** of extreme weather in the next five years.

For problem 2, assess and analysis of various disaster losses caused by high temperatures and droughts in extreme climates, and provide targeted response strategies. This paper chooses **Australia** and **Canada** as two countries to study. First, **DLHDI indicators** are established to show the effects of extreme climates on high temperatures and droughts. Then, based on the indexes of **Drought Index** and **Heat Wave Index in Demarton**, an **Evaluation Model for Heat and Drought losses with double-layer TOPSIS (TOPSIS-HDEM)** is established.The **DLHDI index** values of the two countries were **10.61** and **11.74**, respectively, and the corresponding strategies were put forward according to the results. Finally, we use **Cellular Automata** to simulate Australia and Canada to **verify the robustness of the model**.

For problem 3, assess and analyze the losses caused by flooding and waterlogging in extreme climates, and provide targeted response strategies. In this paper, **China** is selected as the research object. First, **DLFI** is established to **quantify the loss index caused by floods**. Then, water body is extracted based on **remote sensing high-resolution image** and **U-Net network** to assist in floods research. U-Net network selects pre-trained 300-epoch network, and remote sensing image is from GF-2 satellite. Then, this paper establishes **a Floods Disaster Assessment Model based on U-Net (FDAM-UNet)** high-minute two water body extraction to assess floods damage under extreme climatic events, and obtains the **DLFI index** value of **12.71**. Finally, according to the results of the model, specific strategies are put forward.

For problem 4, this report is based on the results of the above studies. The impact and loss assessment of extreme climate, high temperature and drought caused by extreme climate, and flood and waterlogging caused by extreme climate are analyzed and discussed respectively, and corresponding measures are given in the report.

Finally, **sensitivity of the model** established in this paper is analyzed. The calculation shows that the fluctuation of the model is kept **within 5%**, so the model established in this paper is robust and can be used to solve real problems in life.

Keywords: Extreme Climate Disasters, ECPM-THNN Model, TOPSIS-HDEM Model, FDAM-UNet Model, Cellular Automata, RHE Model, Chi-square Coefficient, Matlab

Contents

1. Introduction

1.1 Background

This year, many cities in southern China experienced hot weather for many days, while some parts of the north also witnessed large-scale heavy rainfall. In addition, many European countries have also experienced drought disasters rarely seen in history. Whether it is the hot weather in the south, the heavy rainfall in the north, or the dry weather in Europe, it is unprecedented in decades. Similarly, heavy rainfall has led to a significant reduction in agricultural production in some areas in the north, or even no harvest.

The meteorological department attributed this high temperature phenomenon and heavy precipitation event to the triple La Niña event. The latest data from the World Meteorological Organization shows that the La Niña incident, which has lasted for a long time, is likely to last until the end of this year or later. In June, the British magazine Nature warned that more La Niña events would have multiple impacts, such as increasing the possibility of flooding in Southeast Asia, increasing the risk of drought and wildfire in the southwestern United States, forming multiple hurricanes, cyclones and monsoon patterns in the Pacific and Atlantic, and triggering weather changes in other regions.

(a) Hurricane Event

(b) Wildfire Event

(c) Flood Event

(d) Drought Event

Figure 1: Triple La Niña Event Display

1.2 Restatement of the Problem

Considering the background information and restricted conditions identified in the problem statement, we need to solve the following problems:

- Conduct statistical analysis of the major countries and regions involved in the global Triple La Niña events, and predict the possibility of the Triple La Niña events in the future.
- Taking a country as an example, evaluate and analyze the various types of disaster losses caused by heat and drought under the Triple La Niña event, and provide targeted coping strategies.
- Taking a country as an example, evaluate and analyze various disaster losses caused by floods under the action of the Triple La Niña event, and provide targeted coping strategies.
- Please write a report of no more than 2,000 words for the relevant management in response to the Triple La Niña Event.

2. Problem analysis

2.1 The Analysis and Countermeasures of Problem 1

To address question 1, statistical analysis of the major countries and regions of Triple La Niña events is conducted to predict the likelihood of future Triple La Niña events. Firstly, this paper identifies the factors associated with Triple La Niña events in the Pacific and Central Ocean related regions for model construction. At the same time, the impact indicators of Triple La Niña are selected as the output of the model to study the impact of Triple La Niña in the Pacific and Central Ocean related countries and regions. Then the indicators of the probability of Triple La Niña events are constructed and correlation analysis of the above selected indicators is performed using the chi-square coefficient and Pearson correlation coefficient. Finally, a two-layer Hopfield neural network is used to predict the probability of occurrence of Triple La Niña events and sensitivity analysis is performed on the predicted results.

2.2 The Analysis and Countermeasures of Problem 2

To address question 2, countries are selected for the study to assess and analyze the various disaster losses caused by heat and drought under Triple La Niña and provide targeted response strategies. This paper selects two countries, Australia and Canada, for the study. Firstly, this paper quantifies the impacts caused by heat and drought, and establishes DLHDI indicators to represent the impacts of heat and drought caused by Triple La Niña. Then, we develop a two-layer TOPSIS-based HD-TLN model to assess the damage caused by heat and drought, and provide targeted response strategies based on the model's evaluation results. Finally, the model and the results obtained are validated by simulating a region in Australia and Canada using a meta-cellular automaton.

2.3 The Analysis and Countermeasures of Problem 3

To address question 3, the country is selected as the study target to assess and analyze the various disaster losses caused by floods under the effect of Triple La Niña event and to provide targeted response strategies. In this paper, we select the country of China and take Wuhan, Hubei as the research object, and firstly establish the quantitative damage index DLFI caused by floods, and then establish the F-TLN model based on the U-Net High Score II water body extraction assistance to assess the disaster losses caused by floods, and also assess the disasters caused by floods based on the results obtained from the model.

2.4 Overall Analysis of Problems

For this study on the evaluation of damage and response strategies of extreme climate disasters under the effect of Triple La Niña event, this paper combines the analysis of the above three issues to construct and analyze the framework of the whole paper here.

- ✧ Firstly, In this paper, the factors associated with Triple La Niña events in the Pacific and Central Ocean related regions are identified for model construction. Then the indicators of the probability of occurrence of Triple La Niña event are constructed and correlation analysis of the above selected indicators is performed using the chi-square coefficient and Pearson correlation coefficient. Finally, a two-layer Hopfield neural network is used to predict the probability of occurrence of Triple La Niña events and the sensitivity analysis of the predicted results is performed.
- ✧ Secondly, In this paper, we quantify the impacts of high temperature and drought and establish DLHDI indicators to represent the impacts of high temperature and drought caused by Triple La Niña. This paper then develops a two-layer TOPSIS-based HD-TLN model to assess the damage caused by heat and drought, and provides targeted response strategies based on the model's assessment results. Finally, the model and the results obtained are validated by simulating a region in Canada and Australia using a meta-cellular automaton.
- ✧ Finally, This paper selects the country of China and takes Wuhan, Hubei as the research object. Firstly, we establish the quantitative damage index DLFI caused by floods, and then establish the F-TLN model based on the U-Net High Score II water body extraction assistance to evaluate the disaster damage caused by floods, and also evaluate the disaster caused by floods according to the results obtained from the model and give the corresponding targeted solution measures.

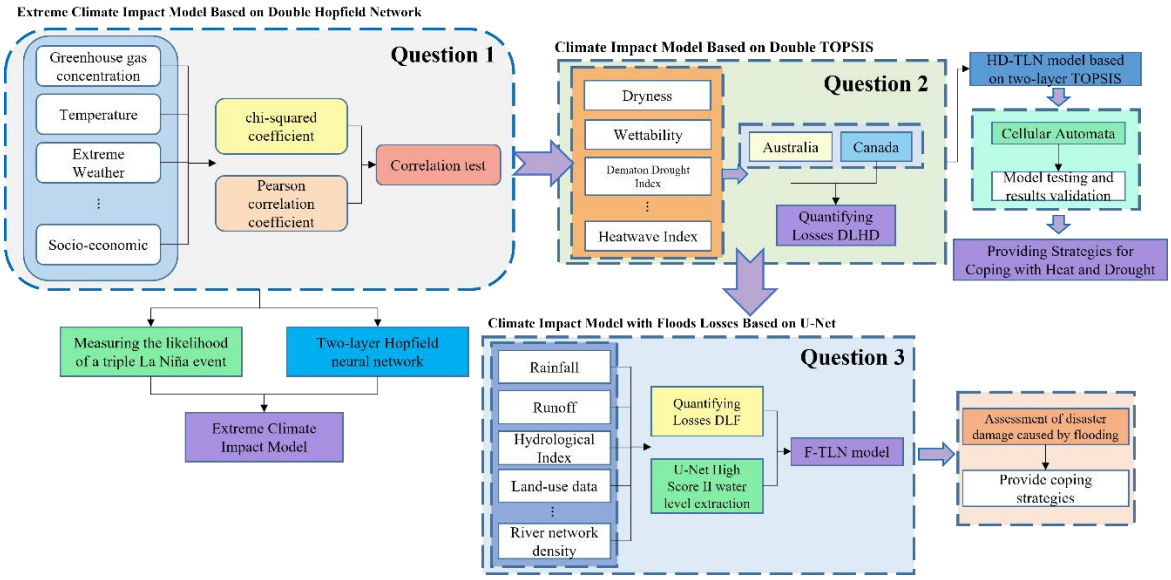

Figure 2: The Backbone of Model

3. Symbol and Assumptions

3.1 Symbol Description

The key mathematical notations used in this paper are listed in **Table 1**.

Table 1: Notations used in this paper

Symbol	Description
TLNI	Metrics related to measuring Triple La Niña events
DLHDI	Indicators to measure damage due to heat and drought
DLFI	Indicators to measure damage caused by floods
P	Indicators to measure the impact of Tirple La Niña
E	Indicators to measure the impact of extreme weather
y_i	Standardized values of global climate change evaluation indicators
d_i	Annual variation of impact factor i
σ_i	Standard deviation of the ith impact factor
w_i	Weight of each impact factor determined by the entropy weighting method

3.2 Fundamental assumptions

To simplify the problem, we make the following basic assumptions, each of which is properly justified.

- **Assumption 1: All countries have responded positively to climate change and taken effective human intervention measures.**
- **Justification:** This paper assumes that all countries will actively respond to the impact of extreme climate change, so as to maintain and promote the rationality

and scalability of the model established in this paper.

- **Assumption 2: The productivity and social structure of each country will not change in the short term studied in this paper.**
- **Justification:** In the research process of this paper, the model established is closely related to each research area. Therefore, for the follow-up study of the problem, it is assumed that productivity and social structure will not change in a short time.

- **Assumption 3: The political form of all countries in the world is relatively stable, and there will be no large-scale war.**
- **Justification:** When studying the impact of extreme climate disasters, this paper does not consider the political forms of countries around the world, so that the research model can fully tap the impact of extreme climate rather than the impact of other uncontrollable factors.

4. Model building and solving

4.1 Model I: Triple La Niña Extreme Climate Impact Model Based on Double Hopfield Network

4.1.1 Problem Description and Analysis

In this paper, we need to statistically analyze the major countries and regions of Triple La Niña events and predict the likelihood of future Triple La Niña events. Firstly, this paper identifies the factors associated with Triple La Niña events in the Pacific and Central Ocean related regions for model construction. At the same time, the impact indicators of Triple La Niña are selected as the output of the model to study the impact of Triple La Niña in the Pacific and Central Ocean related countries and regions. Then the indicators of the probability of Triple La Niña events are constructed and correlation analysis of the above selected indicators is performed using the chi-square coefficient and Pearson correlation coefficient. Finally, a two-layer Hopfield neural network is used to predict the probability of occurrence of Triple La Niña events and sensitivity analysis is performed on the predicted results.

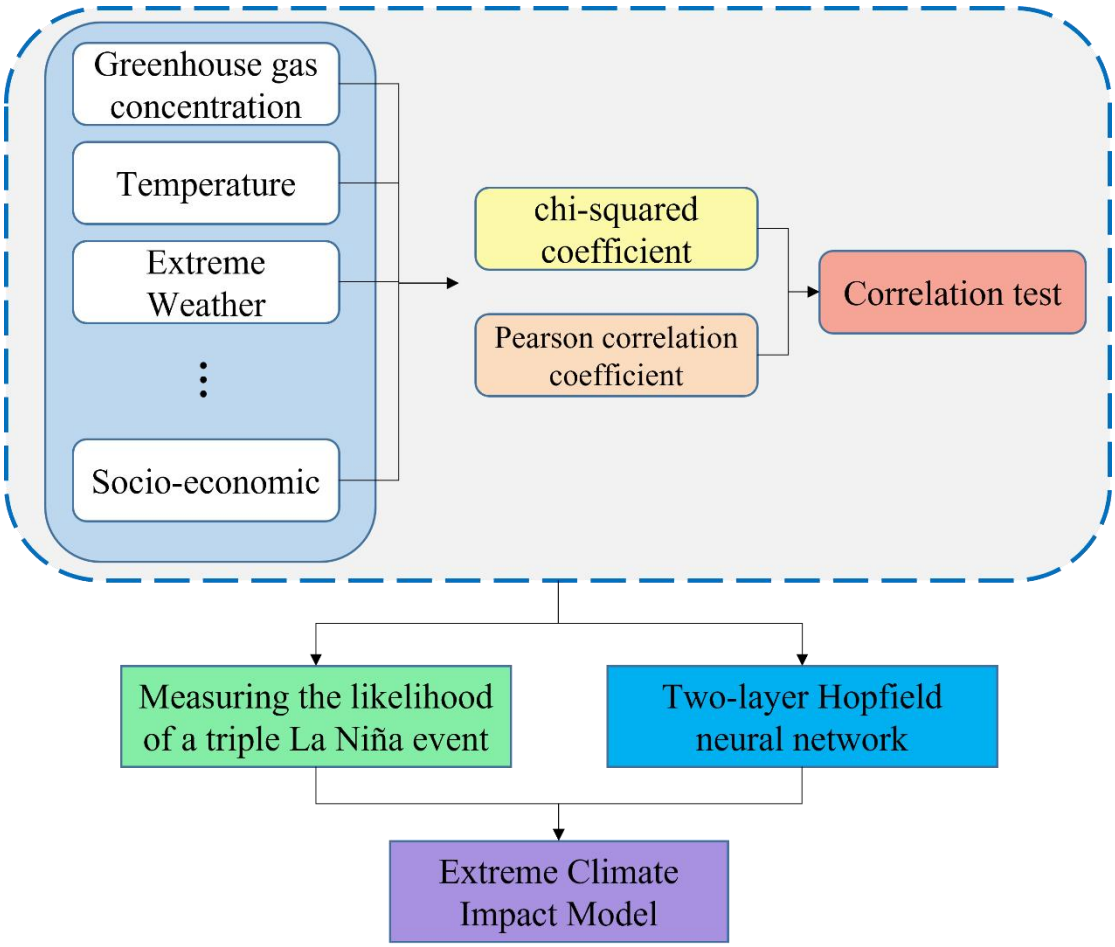

Figure 3: Thought diagram of Question 1

4.1.2 Data Preprocessing

Firstly, for the impact of extreme climate in Triple La Niña on the study area, this paper first collects relevant data, which is done through the relevant URL(https://www.ncei.noaa.gov/maps/daily/) in the title. The main indicators of extreme climate impacts are greenhouse gas concentrations, temperature, extreme weather index, sea level, ocean warming and acidification index, glacier retreat, and melting ice accumulation. In the process of data collection, it was found that there would be missing cases above individual indicators, and some of their missing data are shown below.

Table 2: Missing data related to extreme weather

Time	Greenhouse gas concentration	Sea level index	Glacier retreat index	Ocean warming index	Ocean acidification index
2021	8.35	7.00	8.66	10.11	19.1
2020	8.30	6.91	8.51	9.73	18.7
2019	8.21	6.84	8.44	--	18.6
2018	7.97	6.74	8.37	7.44	18.1
2017	--	6.77	8.23	7.54	17.9

2016	7.83	6.61	--	7.31	17.9
2015	7.79	6.57	8.17	7.22	18.1
2014	7.68	6.44	8.04	7.27	17.6
2013	7.57	6.31	7.91	7.15	18.3
2012	7.41	--	7.88	7.11	18.4
2011	7.55	6.28	7.67	6.98	17.5
.....	.....	.....	.....	.....	.....

For the above missing data, interpolation is performed without affecting the data integrity and the accuracy of the model rationality. The traditional interpolation methods are Lagrange interpolation and Newton interpolation, which require the interpolation polynomials to have equal function values with the interpolated function at the interpolation nodes, but this interpolation method cannot fully reflect the shape of the interpolated function.

Let the function f(x) on the interval [a, b] have n+1 mutually exclusive nodes $a = x_0 < x_1 < x_2 < \ldots < x_n = b$, the function f(x) defined on [a, b] satisfies the following relation on the nodes:

$$f(x_i) = y_i, f'(x_i) = y_i' \ (i=1,2,...,n) \tag{1}$$

A polynomial $H_{2n+1}(x) = H(x)$ with a number not exceeding 2n+1 can be uniquely determined and satisfies:

$$H(x_i) = y_i, H'(x_j) = m_j' \ (j=0,1,2,...,n) \tag{2}$$

The remaining item is:

$$R(x) = f(x) - H(x) = \frac{f^{(2n+2)}(\varepsilon)}{(2n+2)!}\omega_{2n++2}(x) \tag{3}$$

All the missing data were processed according to the above Elmet interpolation method, and some of the results are shown below:

Table 3: Pre-processing of extreme weather-related data

Time	Greenhouse gas concentration	Sea level index	Glacier retreat index	Ocean warming index	Ocean acidification index
2021	8.35	7.00	8.66	10.11	19.1
2020	8.30	6.91	8.51	9.73	18.7
2019	8.21	6.84	8.44	8.71	18.6
2018	7.97	6.74	8.37	7.44	18.1
2017	7.91	6.77	8.23	7.54	17.9
2016	7.83	6.61	8.21	7.31	17.9
2015	7.79	6.57	8.17	7.22	18.1
2014	7.68	6.44	8.04	7.27	17.6
2013	7.57	6.31	7.91	7.15	18.3

2012	7.41	6.30	7.88	7.11	18.4
2011	7.55	6.28	7.67	6.98	17.5
.....	.....	.....	.....	.....	.....

4.1.3 Establishment of Triple La Niña Model and Index

According to relevant studies, the core impacts of extreme climate change are mainly focused on global temperature warming, sea level rise, precipitation anomalies and extreme weather conditions. Therefore, based on these factors, this paper numerically measures the trends of global climate change and extreme weather conditions, and uses the extreme climate change index (TLNI) to measure them, and then models and analyzes these indicators mentioned above.

Extreme climate characteristics, such as temperature, precipitation, or sea level, vary greatly for a country due to its longitude, latitude, and altitude. Therefore, this paper defines the annual temperature difference d_1, the annual precipitation difference d_2, and the annual sea level difference d_3, while their corresponding standard deviations are noted as σ_1, σ_2, and σ_3, respectively.

In this paper, we assume that the temperature, precipitation and sea level indices obey segmented distribution, and we can conclude that the climate has changed when the difference value d_i of a country exceeds the 30-year standard deviation σ_i, which is expressed as follows:

$$\varphi_i = \begin{cases} e^{a|d_i|} - 1, 0 \le |d_i| < \sigma_i \\ b|d_i| + c, \sigma_i \le |d_i| < 2\sigma_i \\ hln(|d_i|) + k, 2\sigma_i \le |d_i| < 5\sigma_i \end{cases} \tag{4}$$

Where φ_1, φ_2 and φ_3 denote temperature, precipitation and sea level index, respectively. Since the functions constructed by the above equations are continuous, it is equivalent that the values of the critical points of the functions are equal. Next, the boundary conditions are given in this paper as follows:

$$\begin{cases} e^{a\sigma_i} - 1 = b\sigma_i + c = 0.1 \\ 2b\sigma_i + c = hln(2\sigma_i) + k = 0.5 \\ hln(5\sigma_i) + k = 1 \end{cases} \tag{5}$$

For the formula established above, the paper presents the difference values as horizontal coordinates and the values measuring climate change as vertical coordinates as follows:

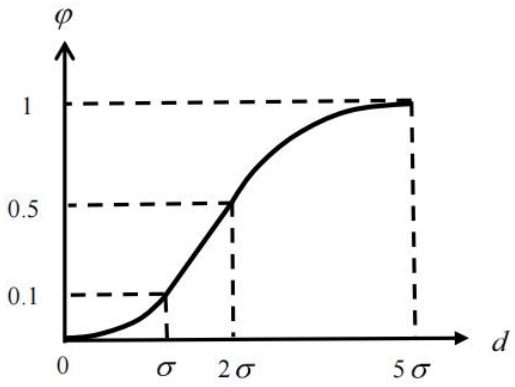

Figure 4: Temperature, precipitation and sea level related indicators

For the variance value d_i, it is reasonable and common for it to vary within the standard deviation range, which is caused by data perturbations whose response is manifested in climate as a result of uncertainties in temperature, precipitation and sea level. Combined with the above figure, the values in equation (1) are set in this paper with the following expressions:

$$\varphi_i = \begin{cases} e^{\frac{ln1.1}{\sigma_i}|d_i|} - 1, 0 \le |d_i| < \sigma_i \\ \frac{0.4}{\sigma_i}|d_i| - 0.3, \sigma_i \le |d_i| < 2\sigma_i \\ \frac{0.5}{ln2.5} ln(|d_i|) + 1, 2\sigma_i \le |d_i| < 5\sigma_i \end{cases} \tag{6}$$

Based on the indicators of temperature, precipitation, and sea level presented above, this subsection discusses the relationship of extreme weather indicators to the measurement of global climate change. According to the relevant literature, extreme weather hazards are mainly reflected in abnormally rare situations such as high temperatures and heavy rainfall. Combined with the indicator model developed in the previous subsection, this paper constructs the extreme weather index TLNI.

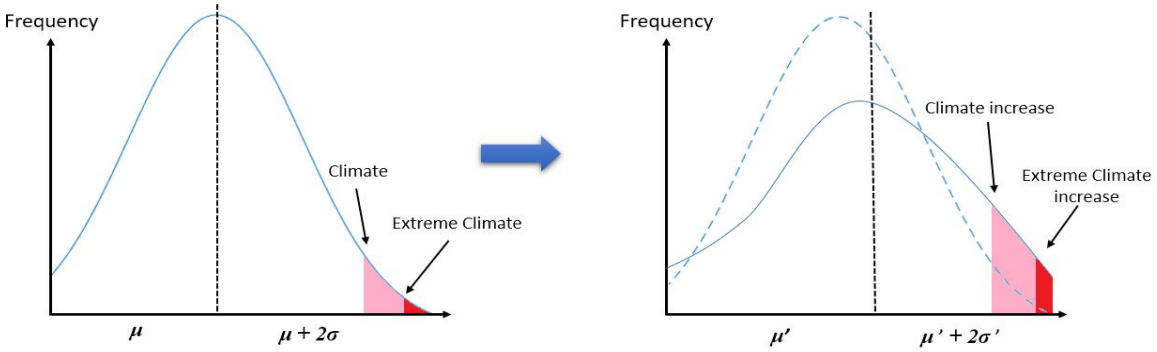

Figure 5: Normal distribution of extreme weather

First, this paper assumes a normal distribution of temperature and precipitation in each country over the year, and thus has the expression:

$$f(t) = \frac{1}{\sqrt{2\pi}\sigma_i} e^{\frac{(t-\mu_i)^2}{2\sigma_i^2}} \tag{7}$$

Where $f(t)$ is the probability density function of temperature, t is the daily average temperature of a region, and μ_i is the annual average temperature. Then this paper defines that the weather is anomalous when the anomaly value is more than twice the standard deviation. The probability function of temperature anomaly is obtained as:

$$P(t) = \int_{\mu_i+2\sigma_i}^{\infty} f(t)dt, P(p) = \int_{\mu_i+2\sigma_i}^{\infty} f(p)dp \tag{8}$$

Thus, according to the above equation, the expression of the extreme weather index TLNI is shown as follows:

$$TLNI = P(t) + P(p) = \int_{\mu_i+2\sigma_i}^{\infty} f(t)dt + \int_{\mu_i+2\sigma_i}^{\infty} f(p)dp \tag{9}$$

In this paper, in order to simplify the model and at the same time improve its effectiveness, we choose temperature, precipitation, sea level anomalies and extreme hazards as the focus to analyze the impact of global climate change. The equation above then models a broader range of first-order indicators, which are then weighted and integrated into a composite indicator that is responsive to changes in climate extremes. Also to facilitate the problem discussion, this paper considers that these factors play an equal degree of influence in the problem solving process, and therefore sets them to the same weight.

$$TLNI = \frac{1}{m}(T + P + \lambda L + E) \times 100 \tag{10}$$

Where $TLNI$ is a measure of extreme climate change, T is a temperature indicator, P is a precipitation indicator, L is a sea level indicator, and E is a glacier retreat indicator.

4.1.4 Establishment of Triple La Niña Extreme Climate Probability Model Based on Double Hopfield Network

Based on the description in the above subsection, the statistical analysis of extreme climate events is characterized in this subsection and the probability of their occurrence is predicted using a two-layer Hopfield neural network. The extreme climate change indicator is used as the energy function of the neural network, and each indicator that affects the extreme climate change is used as the connection layer of the network to train the network. In this way, it is known from the stability theory of continuous Hopfield neural network that when the energy function of the network is stable, the prediction of the probability of occurrence of extreme climate events is also derived.

In this paper, the model is established by analyzing the neurons and neural networks. Artificial neural networks can be divided into feed-forward and feed-back according to the information flow, and the two-layer Hopfield neural network (CHNN) used in this paper belongs to the feedback neural network, which is suitable for dealing with the prediction problem, and the following figure shows the structure of the feedback neural network:

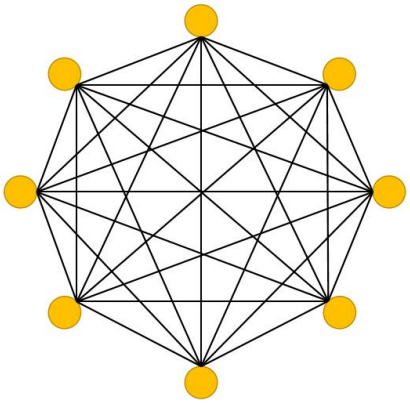

Figure 6: Feedback neural network structure

The mapping of the extreme climate scenario prediction problem into a two-layer Hopfield neural network is divided into the following main steps:

1、Design of permutation matrix under CHNN model

Figure 7: Hopfiled network mapping step-by-step diagram

To map the extreme climate prediction problem as a dynamic process of a neural network, the NN model is constructed. Each extreme climate indicator is corresponding to each neuron of the neural network. Each row and column has only one 1 and the rest are 0. The sum of 1's in the matrix is N. The matrix is then called the permutation matrix.

2、Constructing the network energy function and dynamic prediction equation

For the climate situation prediction problem, on the basis of the CHNN energy function, the following two issues need to be considered to design the predicted energy function.

(1) The rules of the translation substitution matrix that need to be quantified for planning the predicted energy function.

(2) Among the multiple outcomes in the prediction problem, the energy function should facilitate the quantitative representation of the accuracy of the prediction.

The energy function of the neural network contains two parts: the target term and the constraint term, where the target term is the objective function corresponding to the energy function, and the constraint term is the permutation matrix.

Because the energy function is too complex, drawing on the experience of previous people in prediction of the energy function, the energy function is improved as follows:

$$E = \frac{A}{2}\sum(\sum v_{ij} - 1)^2 + \frac{A}{2}\sum(\sum k_{ij} - 1)^2 \quad (11)$$

Also for V, which is the set of system output state variables:

$$V = \{v_i(t)|i = 1,2,\ldots,N\} \quad (12)$$

3、The initialization and iterative optimization of the CHNN Hopfield neural network iterative process is very sensitive to the coefficients of the energy function and dynamic equations. Therefore, the network input initialization is selected as follows:

$$U_{xi}(t) = \frac{1}{2}U_0 ln(n-1) + \delta_{xi} \quad (13)$$

Where the value of U_0 is 1 and n is the number of days. After initializing the network, the network is trained. The training process includes the calculation of dynamic equations, input and output neuron state updates and the calculation related to the energy function. When the structure and parameters of CHNN are designed, the prediction process will become easy. The specific steps are as follows.

Step1: Import the actual value of the pass rate into the neural network for initialization of the network.

Step2: Use the dynamic equation to calculate

$$\frac{du_{xi}}{dt} \quad (14)$$

The input state of the neural network at the next moment is calculated by the first-order Eulerian method with the following equation:

$$U_{xi}(t+1) = U_{xi}(t) + \frac{dU_{xi}}{dt}\Delta t \quad (15)$$

Step3: The Sigmoid function is often used as the activation function of a neural network, mapping the variables between [0, 1]. Therefore, the output state of the neural network at the next moment is updated according to the Sigmoid function, with the following equation.

$$V_{xi}(t) = \frac{1}{2} + tanh(\frac{U_{xi}(t)}{U_0}) \quad (16)$$

Where the tanh activation function is a modified version of the Sigmoid function.

Step4: Using the energy function calculation, the training calculation of Hopfiled neural network is ended after the training reaches a predetermined number of times.

According to the above description, firstly, the countries and regions where extreme climate change occurs globally are counted and the indicators are shown below:

Table 4: Indicator Data Presentation for Extreme Climate Impact Countries

Countries	China	Australia	Indonesia	Brazil	India	Canada	America
TLNI	12.5	13.1	12.7	11.5	12.6	13.2	12.8

The above are the scores calculated by the extreme climate analysis model established in this paper, in which it is found that the extreme climate studied in this paper is indeed closely related to the countries adjacent to the Pacific Ocean. Then the probability of future climate extremes in these countries and regions is predicted using a two-layer Hopfield neural network, and the results are shown below:

Table 5: Analysis and prediction of extreme weather

Country	2023-Possibility	2024-Possibility	2025-Possibility	2026-Possibility	2027-Possibility
China	0.17	0.18	0.05	0.07	0.04
Australia	0.15	0.14	0.08	0.05	0.05
Indonesia	0.18	0.15	0.04	0.06	0.07
Brazil	0.14	0.14	0.07	0.08	0.06
India	0.16	0.16	0.04	0.04	0.05
Canada	0.15	0.17	0.05	0.05	0.08
America	0.17	0.15	0.08	0.07	0.07

The above results, on the other hand, are predictions based on extreme climate indices, along with an error analysis of the two-layer Hopfield network, which is shown in the following figure:

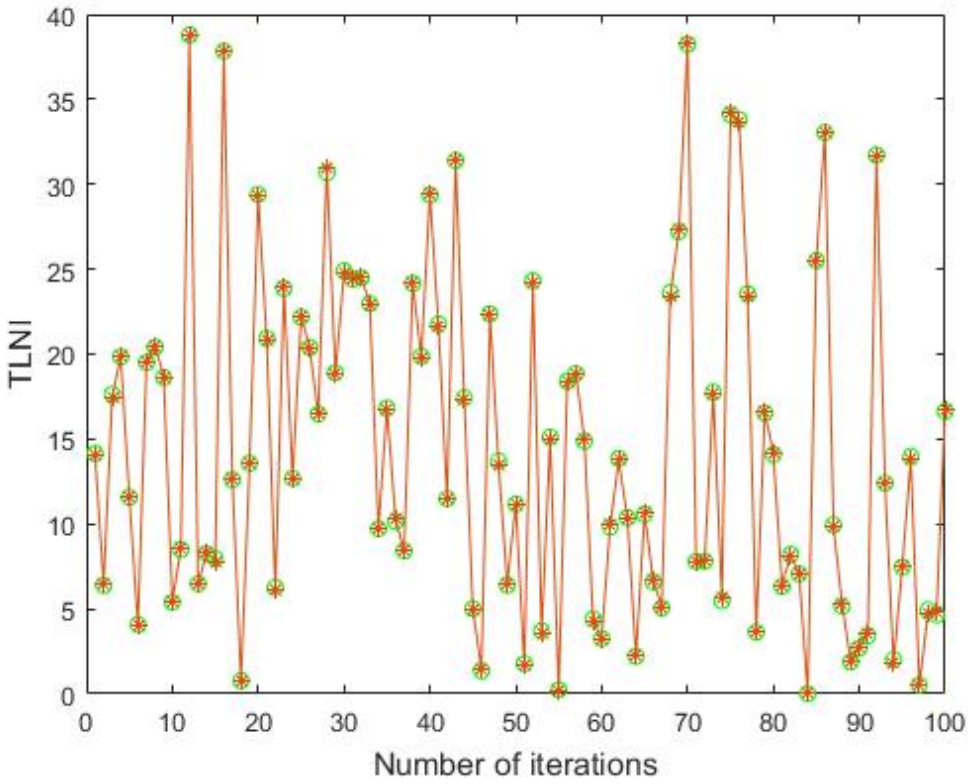

Figure 8: Double-layer Hopfield network error analysis diagram

Using the above figure and after calculating the error, it is found that it is feasible to use the two-layer Hopfield neural network for extreme climate prediction. The error

of the two-layer Hopfield neural network is 6.91%, so it can be considered that the two-layer Hopfield neural network can predict TLNP accurately.

4.2 Model II: Triple La Niña Climate Impact Model with Heat and Drought Losses Based on Double TOPSIS

4.2.1 Problem Description and Analysis

In this paper, we need to select countries for the study to assess and analyze the various disaster losses caused by heat and drought under Triple La Niña and provide targeted response strategies. This paper selects two countries, Australia and Canada, for the study. Firstly, this paper quantifies the impacts caused by heat and drought, and establishes DLHDI indicators to represent the impacts of heat and drought caused by Triple La Niña. Then, we develop a two-layer TOPSIS-based HD-TLN model to assess the damage caused by heat and drought, and provide targeted response strategies based on the model's evaluation results. Finally, the model and the results obtained are validated by simulating a region in Somalia and Mexico using a meta-cellular automaton.

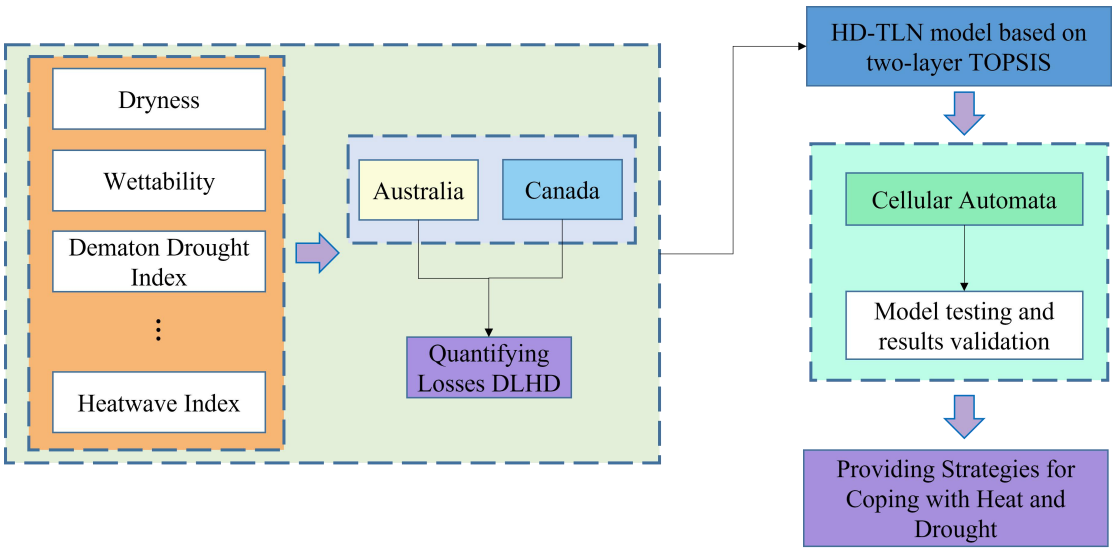

Figure 9: Thought diagram of Question 2

4.2.2 Establishment of Triple La Niña Losses Index

In this paper, we describe the representation of the extreme climate indicator TLNI and use it to construct a model to analyze the possibility and extent of extreme climate. In order to measure the impact of extreme climate on heat and drought, this paper firstly selects the indicators of heat and drought, and further measures the impact of extreme climate, which is also called DLHDI. and briefly introduce these indexes.

①Dryness X_1: The impact of high temperature and drought caused by extreme climate can be measured by using dryness, so it can be used as one of the indicators.

②Wetness X_2: The impact brought by high temperature and drought brought by

extreme climate can be expressed by using wetness, while wetness can better reflect the impact brought by extreme climate, so it can be used as one of the indicators.

③ Dematon drought index X_3: Dematon drought index can well reflect the impact brought by extreme climate on drought, so it is very suitable as an indicator to measure the impact of extreme climate on drought.

④ Precipitation temperature homogenization index X_4: the precipitation temperature homogenization index can well reflect the information of temperature and humidity, and therefore can be used to measure the impact brought by extreme climate on high temperature and drought.

⑤ Heat wave index X_5: The heat wave index can well reflect the impact caused by high temperature brought by extreme climate, so it is very suitable as an indicator to measure extreme climate.

For the selection of the above indicators, this paper visualizes them as follows:

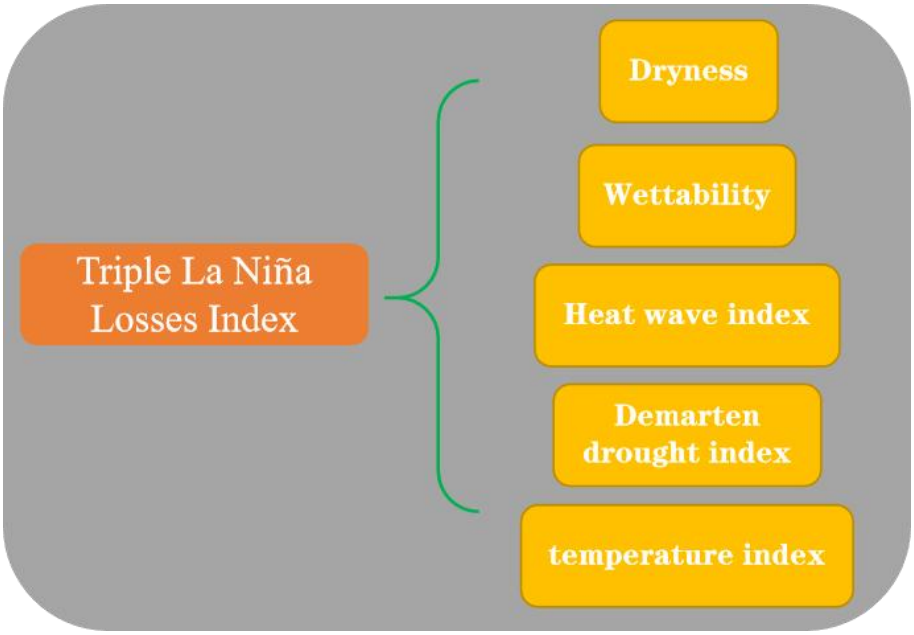

Figure 10: Extreme climate loss index display

After the selection of the above indicators, the determination of the weights is further carried out, and here in this paper the entropy weight method is used for the selection of weights. Considering the influence of positive and negative indicators on environmental pollution indicators, the following equations are available:

$$\begin{cases} y_i = \dfrac{x_i - min(x_i)}{max(x_i) - min(x_i)} \\ y_i = \dfrac{max(x_i) - x_i}{max(x_i) - min(x_i)} \end{cases}, \ i = 1,2,\ldots,5 \tag{17}$$

where y_i represents the standardized values of extreme climate indicators and x_i is the high temperature drought measure.

The standardized values of environmental pollution are then processed as follows:

$$P_i = \frac{y_i}{\sum y_i} \tag{18}$$

After the above processing, according to the definition of information entropy, this paper uses the calculation method of information entropy as follows:

$$E_i = -\sum P_i \, ln(P_i) \tag{19}$$

The weights of each of the previously defined influencing factors are further calculated by means of the information entropy calculation:

$$w_i = \frac{1 - E_i}{k - \sum E_i}, \; i = 1,2,\ldots,5 \tag{20}$$

According to the above steps, the weights of each influencing factor can be calculated, and then the degree of each influencing factor on the environmental pollution impact model can be measured, and the specific results are shown below:

Table 6: Information entropy weights

Dryness index	Wettability index	Heat wave index	Demarten drought index	temperature index
0.2213	0.1914	0.1732	0.2142	0.1999

Through the above selection of factors related to extreme climate related to high temperature and drought influence, the correlation between the selected indicators will be calculated next. Firstly, the base matrix M is calculated in this paper as shown below:

$$M = \begin{pmatrix} m_{11} & m_{12} & \cdots & m_{1n} \\ m_{21} & m_{22} & \cdots & m_{2n} \end{pmatrix} \tag{21}$$

Based on the values of the matrix above, the cardinality is calculated as follows:

$$\chi^2 = g\left(\sum\sum\left(\frac{m_{ij}^2}{g_2 g_n}\right) - 1\right) \tag{22}$$

Where $g = \sum\sum m_{ij}$, the Pearson correlation coefficient can then be calculated, and the formula is shown below:

$$C = \sqrt{\frac{\chi^2}{(g + \chi^2)}} \tag{23}$$

Where the larger value of C indicates the closer correlation between the indicators, the correlation between the indicators mentioned above is judged by the standard error SE through the least squares method of solution estimation using the formula above. Where the specific expression of SE is as follows:

$$SE = \sqrt{\frac{\sum (f_i(X_i) - \widehat{f}_i)^2}{n - 3}} \tag{24}$$

For the determination of the above correlations, significance tests were done and the results are shown below:

Table 7: Demonstration of correlation between extreme climate heat and drought indicators

Model	Sum of Squares	Degrees of Freedom	Mean Square	F	Significance
Regression	15378.278	9	1098.451	23.814	0.000132
Residuals	4332.521	48	46.088		
Total	19710.571	57			

From the above table, it can be concluded that the indicators selected in this paper can well reflect the relationship between extreme climate on high temperature and drought. The next step is to build a model to measure the impact of high temperature and drought under extreme climate based on the above established metrics.

4.2.3 Establishment of Triple La Niña Extreme Climate Losses Analyze Model Based on Double TOPSIS

Based on the extreme climate related impact indicators of high temperature and drought established in the previous subsection, the extreme climate model of high temperature and drought based on two-layer TOPSIS is established in this subsection, and this paper uses the two-layer TOPSIS comprehensive evaluation method to assess the damage caused by high temperature and drought, and provides targeted response strategies based on the obtained results. This paper assesses the damage caused by high temperature and drought in extreme climates based on the basic idea of TOPSIS evaluation, and its assessment steps are as follows:

Step1: Isotropization and standardization of the indicators, and then obtaining the weights by the entropy weighting method, which avoids the influence of subjective factors, while obtaining the weight vector and the standardization matrix.

Step2: The weighted normalized matrix is obtained with the following expressions:

$$Z = (z_{ij})_{n\times m} = (p_{ij} \times w_{ij}) \tag{25}$$

Step3: Determining positive and negative ideal solutions, with positive understood as the best value in the indicator that reaches the sample and negative ideal solutions as the worst value in the indicator.

Step4: The distance of each sample from the positive and negative ideal solution is calculated and the formula is shown below:

$$\begin{aligned} D_i^+ &= \sqrt{\sum (z_{ij} - z_j^+)^2} \\ D_i^- &= \sqrt{\sum (z_{ij} - z_j^-)^2} \end{aligned} \tag{26}$$

Step5: The degree of closeness of each secondary indicator to the corresponding primary indicator is calculated with the following formula:

$$C_i = \frac{D_i^-}{D_i^+ + D_i^-} \tag{27}$$

Through the above steps, the evaluation relationships of different new energy use models are obtained, and the expression relationships between the indicators are written accordingly in this paper as follows:

$$\varphi_i = \sum w_{ij}\varphi_{ij} \times C_i, \text{i=1,..,5} \tag{28}$$

Through the above steps, this paper chooses to use the countries of Australia and Canada to carry out the assessment of the loss of extreme climate impact on heat and drought, and proposes the corresponding strategies according to this. Meanwhile, the characteristics of Australia and Canada countries are shown as follows:

Figure 11: Geographical and climatic characteristics of Australia

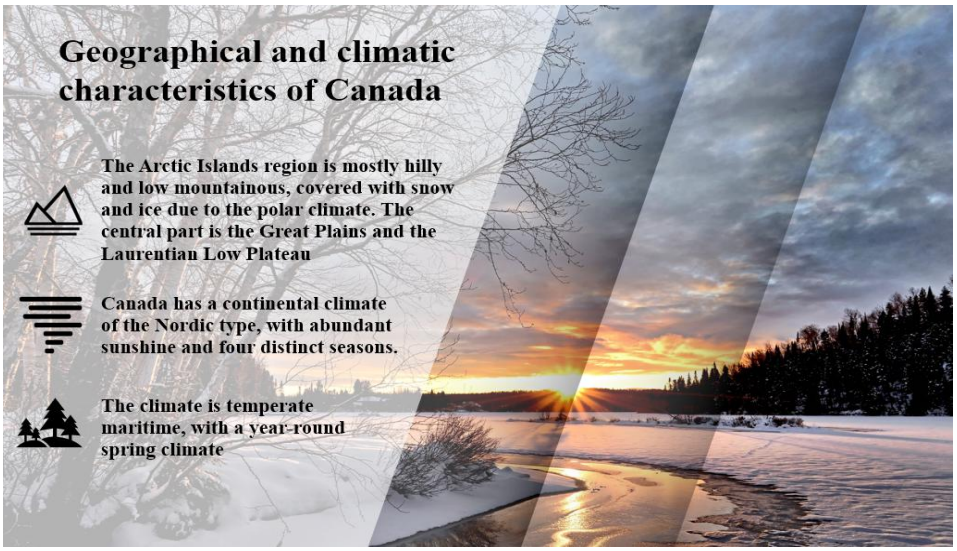

Figure 12: Geographical and climatic characteristics of Canada

The results calculated from the above model are shown below:

Table 8: Loss assessment score for each indicator

Country	Dryness index	Wettability index	Heat wave index	Demarten drought index	temperature index
Australia	5.1	5.7	4.9	4.5	4.9
Canada	6.7	4.9	5.2	5.6	4.7

Based on the above table, this paper uses five indicators to measure the assessment of disaster losses from climate extremes in two countries, Australia and Canada, where these five indicators can reflect two characteristics to be studied, namely high temperature and drought. It can be obtained that both Australia and Canada have been traumatized by climate extremes, especially in terms of heat and drought. Meanwhile, the above table is expressed as follows:

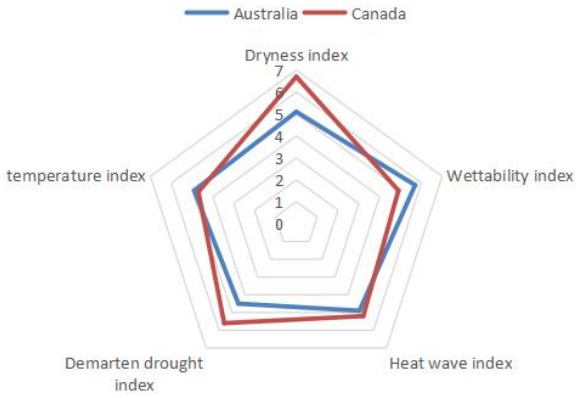

Figure 13: Extreme weather heat and drought damage display

Based on the above table, it can be seen that there are differences and similarities in the effects of climate extremes on Australia and Canada. In particular, the extreme climate brings about high temperatures that affect the temperature homogenization index and the dryness index of both countries, which can lead to reduced cereal yields, droughts, and economic recessions in countries that suffer from extreme weather. In terms of differences, Australia's precipitation is more susceptible to climate extremes, and because of its special geographical location, it is more susceptible to drought than Canada. The geographical location of Canada is more likely to receive the impact of high temperature, and its most productive wheat will also occur due to extreme climate impact of very serious yield reduction, in view of the above analysis, for different countries to take different coping strategies. For the Australian region, water storage can be properly stored and dams and other water storage sites can be built to cope with sudden weather extremes. For Canada, the temperature response can be appropriate to develop local farming techniques, the use of constant temperature greenhouses for crop cultivation, etc.. Although the probability of sudden weather extremes is extremely low, countries should pay attention to this matter in order to be able to deal with the effects of sudden weather extremes comfortably.

4.3 Model III: Triple La Niña Climate Impact Model with Floods Losses Based on U-Net with High Resolution Image Water Body Extraction

4.3.1 Problem Description and Analysis

In this paper, we need to select countries as research subjects to assess and analyze various disaster losses caused by floods under the effect of Triple La Niña event and provide targeted response strategies. In this paper, we select the country of China and take Wuhan, Hubei as the research object. We firstly establish the quantitative damage index DLFI caused by floods, and then establish the F-TLN model based on the U-Net High Score II water body extraction assistance to assess the disaster losses caused by floods, and also assess the disasters caused by floods based on the results obtained from the model.

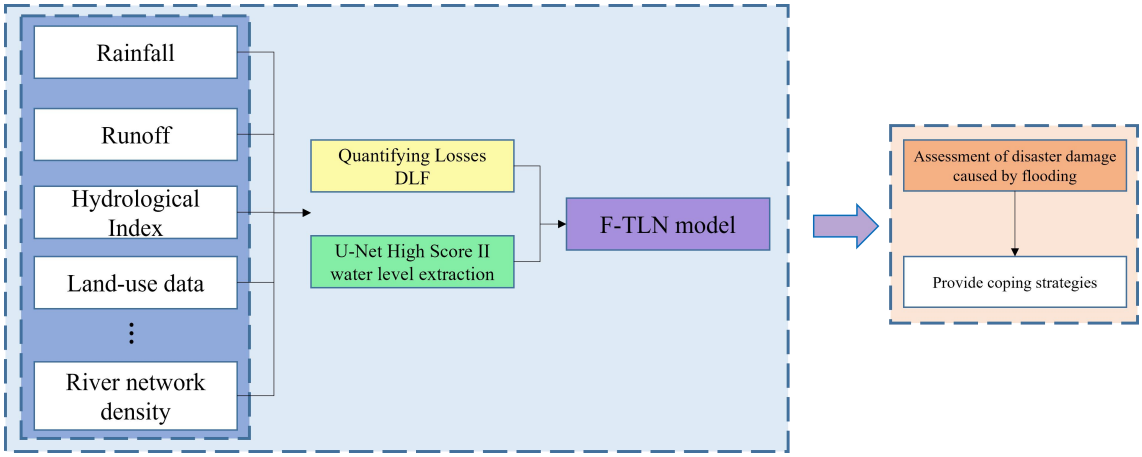

Figure 14: Thought diagram of Question 3

4.3.2 Establishment of Triple La Niña Floods Losses Index

In this subsection, we need to measure the impact of flooding in extreme weather. The following is a brief introduction of these indicators.

① Rainfall Y_1: The impact of flooding caused by extreme weather can be measured using rainfall, so it can be used as one of the indicators.

②Runoff Y_2: The impact of flooding disasters brought about by extreme climate can be expressed using runoff volume, while runoff volume can better reflect the impact brought about by extreme climate, so it can be used as one of the indicators.

③ Hydrological data Y_3: Hydrological data can well reflect the impact of flooding brought about by extreme climate, so it is very suitable as an indicator to measure extreme climate.

④ Vegetation data Y_4: vegetation data can reflect the information of flooding well, so it can be used to measure the impact brought by flooding under the effect of extreme climate.

⑤ Hydrological water level observation point density Y_5: the density of hydrological water level observation points can well reflect the impact caused by

flooding under the effect of extreme climate, so it is very suitable as an indicator to measure extreme climate.

⑥River network density Y_6: The density of river network can well reflect the impact of flooding under the effect of extreme climate, so it can be used as an indicator to measure DLFI.

For the selection of the above indicators, this paper visualizes and represents them as follows:

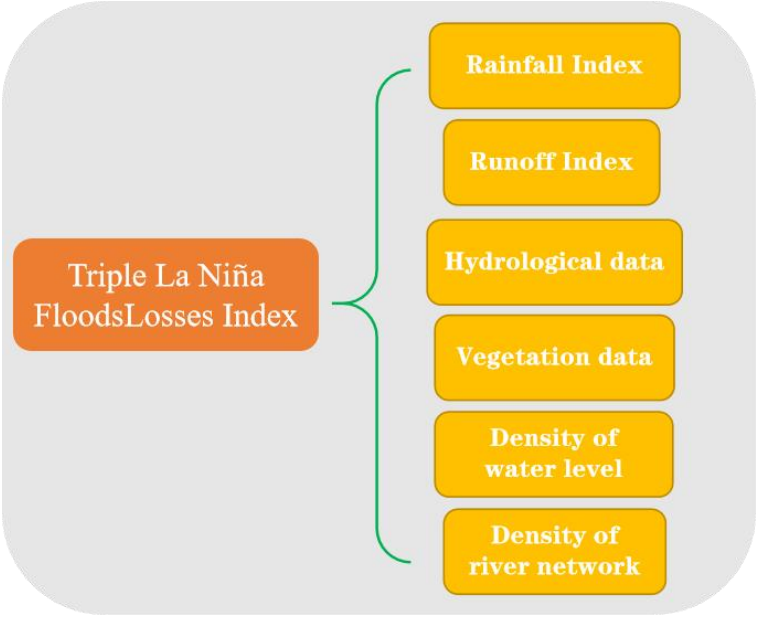

Figure 15: Extreme climate floods loss index display

After the selection of the above indicators, the determination of weights is further carried out, and here in this paper the entropy weighting method is used for the selection of weights. Since the calculation method is the same as that in the previous subsection, the calculation steps are omitted here and the results are given directly.

Table 9: Information entropy weights

Rainfall Index	Runoff Index	Hydrological data	Vegetation data	Density of water level	Density of river network
0.2213	0.1914	0.1732	0.2142	0.0909	0.1090

With the above selection of factors concerning the influence of flooding caused by extreme weather, the correlation between the selected indicators will be calculated next. Again here the calculations are performed according to the method discussed above and the results are given directly.

Table 10: Correlation demonstration of extreme climate flooding indicators

Model	Sum of Squares	Degrees of Freedom	Mean Square	F	Significance
Regression	13378.278	9	1098.451	23.814	0.0072
Residuals	3332.521	45	46.088		
Total	16710.571	54			

From the above table, it can be concluded that the indicators selected in this paper can well reflect the relationship between the indicators of flooding under extreme weather conditions. The next step is to build a model to measure the impact of flooding under extreme weather conditions and to propose corresponding solutions based on the above established indicators.

4.3.3 High-Resolution Water Extraction Based on U-Net

In order to address the problem of assessing the impact of flooding under extreme climate, China is chosen for this paper, and to simplify the complexity of the research problem and to better demonstrate the model building process, Wuhan, Hubei is chosen as a small area for the study of U-Net based water extraction from high resolution images.

First of all, water extraction is a popular research topic in the field of remote sensing and mapping, and has been widely and informatively studied. The water body extraction is gradually converted from the traditional method to the deep learning method, because the deep learning method can better mine the water body feature information, and then the water body can be extracted more quickly and accurately. This paper uses U-Net neural network, which is one of the earlier algorithms using full convolutional network for semantic segmentation, and it uses compressed path and extended path to process the input image. And its name is taken from its U-shaped network shape, and its network results are shown as follows:

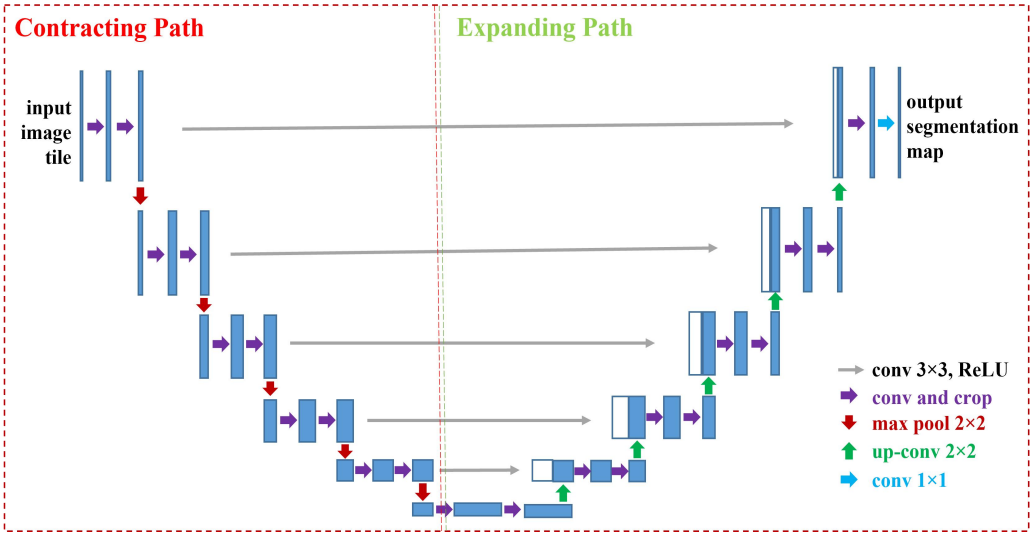

Figure 16: U-Net Network Architecture

Based on the U-Net network used above, this paper selects the Wuhan city area for water body extraction and uses this as the auxiliary information needed for the following modeling, and the results of water body extraction for the Wuhan city study area are shown below.

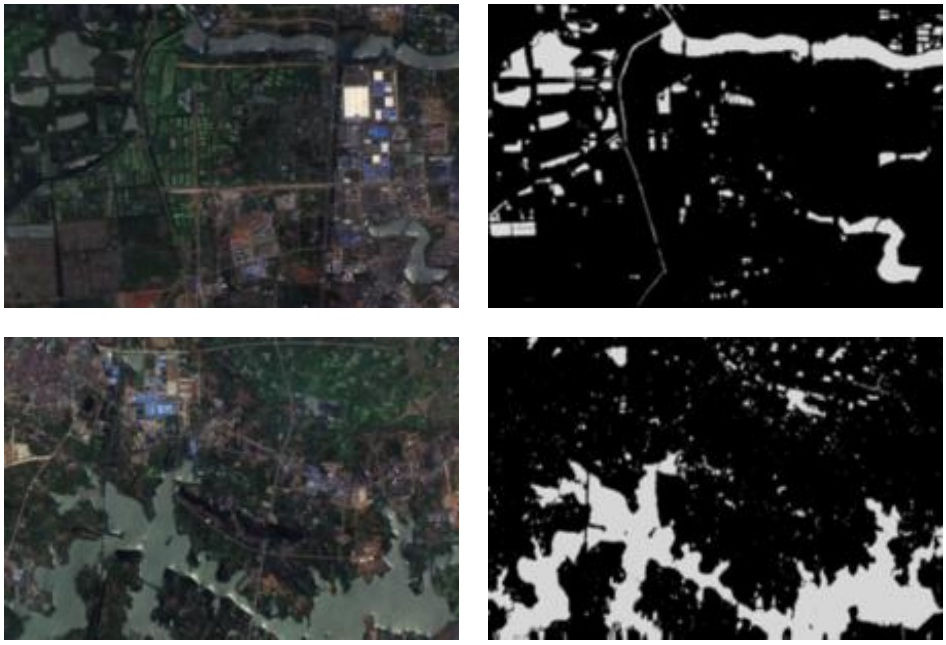

Figure 17: Wuhan City Water Extraction Results

The above is the result of extracting water bodies from Wuhan city data acquired by the HMS-2 satellite, where we obtain three indicators of water bodies, background and semantic, with values of 85.19, 97.88 and 91.53, respectively. This paper intends to use the extraction of water bodies from high-resolution imagery to assist in the study of the effects of extreme weather-induced flooding hazards, and to propose corresponding measures to address them.

4.3.4 Establishment of Triple La Niña Extreme Climate Losses Model Based on U-Net

Based on the impact indicators related to flooding under extreme climate effects established in the previous subsection, an extreme climate model for flood damage assessment based on U-Net high-resolution image aided by water body extraction is established in this subsection. In this paper, flood-related indicators and water body extraction-aided indicators are used to assess the damage caused by flooding, and targeted response strategies are developed based on the obtained results.

In this paper, based on the fact that the indicators of flooding under the effect of extreme climate basically obey normal distribution, the following expressions are available.

$$f(t) = \frac{1}{\sqrt{2\pi}\sigma_i} e^{-\frac{(t-\mu_i)^2}{2\sigma_i^2}} \tag{29}$$

Then this paper defines that when the anomalous value of the flooding index exceeds twice the standard deviation, the impact caused by flooding under extreme climate effects is not negligible, and the probability function of temperature anomaly is obtained as:

$$P(t) = \int_{\mu_i+2\sigma_i}^{\infty} f(t)dt, P(p) = \int_{\mu_i+2\sigma_i}^{\infty} f(p)dp \tag{30}$$

Thus, based on the above equation, the expression for the loss indicator DLFI due to flooding is shown below:

$$DLF = P(t) + P(p) = \int_{\mu_i+2\sigma_i}^{\infty} f(t)dt + \int_{\mu_i+2\sigma_i}^{\infty} f(p)dp \tag{31}$$

In this paper, in order to simplify the model and at the same time improve its effectiveness, the indicators extracted from rainfall, runoff, hydrological data, land use data, and water bodies under high resolution remote sensing imagery are chosen as the focus to analyze the impact caused by flooding under extreme climate. The above equation then weights these indicators and integrates them into a comprehensive indicator, which is able to respond to the changes of extreme climate. Also to facilitate the problem discussion, this paper considers that these factors play an equal degree of influence in the problem solving process, so they are set to the same weight.

$$DLFI = \frac{1}{m}(R + H + V + WBE) \times 100 \tag{32}$$

Among them, *DLFI* is a metric for measuring flooding caused by extreme climate, *R* is rainfall, *H* is runoff, *V* is land use data, and *WBE* is a semantic indicator for water body extraction under high resolution remote sensing imagery.

Through the above steps, this paper chooses to use the country of China for the impact loss assessment caused by flooding under the effect of extreme climate, and proposes the corresponding strategy according to this. The loss score data of each of these indicators are shown as follows.

Table 11: Loss assessment score for each indicator

Country	Rainfall Index	Runoff Index	Hydrological data	Vegetation data	Density of water level	Density of river network
China	6.1	7.7	6.9	5.5	6.9	7.1

Based on the above table, this paper uses the above six indicators to measure the assessment of disaster losses caused by floods in China under extreme weather effects, where these six indicators can reflect the impact caused by floods, while the above table is expressed as follows:

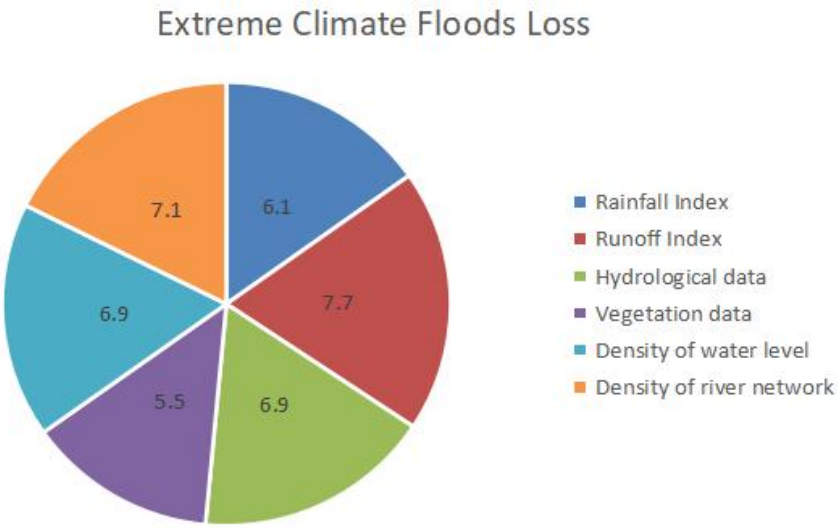

Figure 18: Demonstration of damage from flooding under extreme weather effects

According to the above table, it can be found that the impact of flooding under the effect of extreme climate is more obvious in China. Among them, flooding from extreme climate affects various indicators such as rainfall, runoff, hydrological data, land use data, and vegetation data in China. The results of the U-Net network water extraction in Wuhan, China, show that Wuhan receives flooding in extreme weather conditions, and for the Wuhan study area, farmland and roads are flooded and large areas of standing water are created. If this water is not discharged in time, it will affect the crop yield and even more seriously the economic development of China. In response to the effects of flooding in extreme weather, China should increase its green areas and plant more trees and grasses to improve the land's ability to hold water. For urban areas, China can create sponge cities, which take advantage of the dense construction of underground pipelines in urban areas to improve the capacity and level of urban flood control.

4.4 A Report in Response to the Triple La Niña Event

Triple La Niña is Sneaking into Our World

In the equatorial eastern central Pacific Ocean, there is a "little girl" lurking, when the sea surface temperature continues to be abnormally cold on a wide scale, this "little girl" may appear, her name is "La Niña "The name is La Niña. The emergence of this extreme climate has had a serious impact on many cities in southern China, with many days of hot weather and rare drought disasters exposing southern cities to La Niña. And extreme weather such as heavy precipitation and high temperatures in northern cities will lead to a significant reduction in agricultural production, or even no harvest. Based on the above background, this report analyzes the possibility of extreme weather, the impact of high temperatures and droughts due to extreme weather effects, and the damage caused by floods due to extreme weather effects, and provides a report to the World Meteorological Organization for use in

addressing global extreme weather issues.

To address the issue of La Niña extremes and their likelihood, this report first identifies factors related to La Niña events in the eastern and central Pacific Ocean related regions for model construction. In this report, indicators related to greenhouse gas concentrations, sea level, ocean warming and acidification indices, glacier retreat, and ice accumulation melting are selected for study. At the same time, La Niña impact indicators are constructed to measure the impact of climate extremes, and La Niña impact indicators are selected as model outputs to study the impact of La Niña in Pacific-related countries and regions. Then the indicators of La Niña event probability are constructed and correlation analysis of the above selected indicators is performed using the chi-square coefficient and Pearson correlation coefficient. Finally, using a two-layer Hopfield neural network to predict the probability of La Niña events, it is found that the probability of occurrence in China, Australia, Indonesia, Brazil, India, Canada and the United States is less than 0.2 in the next five years and less than 0.1 after 2025, so it is reasonable to say that people are aware of the impact of extreme weather and have started to take a series of The sensitivity analysis of the predicted results is within 6.91%, which gives reason to believe in the accuracy of the predicted results.

This report selects two countries, Somalia and Mexico, to study the problem of high temperature and drought caused by La Niña extremes. Firstly, this report quantifies the impacts of high temperature and drought caused by extreme weather and establishes DLHDI index to represent them. This report then establishes a two-layer TOPSIS-based extreme weather impact model to assess the damage caused by heat and drought, and calculates the values of dryness index, wetness index, Dematon drought index, and heat wave index, which are 5.1, 5.7, 4.9, 4.5, and 4.9, respectively, based on the results of the model to provide targeted response strategies The results of the model assessment are used to provide tailored response strategies for each country based on its geographical and climatic environment. Finally, this report validates the model and the results obtained by simulating a region in Somalia and Mexico using a meta-cellular automaton.

To address the problem of flooding caused by La Niña extreme climate, this report selects the country of China as the research object, and takes Wuhan, Hubei Province as a more detailed research object, and firstly establishes the quantitative damage index DLFI caused by flooding, and then establishes the F-TLN model based on U-Net High Score II water body extraction assisted to evaluate the disaster damage caused by flooding, and the U-Net network uses 300 Epoch to pre-train and input the images of Hubei Province into the U-Net network for water body extraction. The indicators obtained from the U-Net network were combined with the corresponding indicators from DLFI to analyze the Chinese country. The values of 6.1, 7.7, 6.9, 5.5, 6.9, and 7.1 were obtained for the indicators related to flooding, and the indicators were used to develop preventive measures for flooding caused by extreme weather in China, and to provide measures for flood prevention and control according to the characteristics of different urban areas in China.

In summary, the above is an analysis of La Niña climate extremes related to El Niño and La Niña events as important, but not the only, drivers of the Earth's climate system. Despite the persistence of La Niña events in the east-central equatorial Pacific Ocean, sea level temperatures are estimated to remain generally above average elsewhere. Although the La Niña event is exceptional and its cooling effects have temporarily slowed the rise in global temperatures, to truly protect the Earth's environment for the benefit of future generations, it is still necessary for each of us to start now, build environmental awareness, and implement environmental protection behaviors into our practical lives.

5. Test the Models and Sensitivity Analysis

5.1 Simulation Experiment of Cellular Automata

For the extreme climate-induced heat and drought loss assessment model based on two-layer TOPSIS established in Problem 2, this paper would like to validate the parameters and results of the model by using a cellular automata. Cellular Automata is a lattice dynamics model with discrete time, space, and state, and localized spatial interactions and temporal causality, which has the ability to simulate the spatio-temporal evolution of complex systems.

The cellular automaton consists of a regular lattice of cells, and each cell scattered in the regular lattice takes a finite number of discrete states, follows the same action rules, and makes synchronous updates according to the determined local rules. In this paper, we define its state at moment t as follows:

$$S_t = (E_t, R_t, I_t, \lambda_t, \gamma_t) \tag{33}$$

For the state of the above Cellular Automata at moment t, this paper defines its update rule as follows:

$$S_{t+1} = \varphi(E_t, R_t, I_t, \lambda_t, \gamma_t) \tag{34}$$

Here $\varphi(\cdot)$ is a five-dimensional discrete function that defines the rules of the Cellular Automata and constrains the update rules of the Cellular Automata in each dimension. Also, for the disease transmission model, this paper restricts it to a 01 binary variable. Thus for the above description, there are only 2^5 possibilities for the state change of a tuple from moment t to moment t+1. Also, this paper restricts the possibility of state occurrence to be equal for each position in the specified region.

For the above description, this paper uses the Cellular Automata to simulate some regions of Canada, and in this paper, the two regions are treated as two-dimensional square spatial domains, where each location in the region is replaced by a pixel block, and the pixel blocks of different colors represent different individual states, and the simulation results are shown in the following figure.

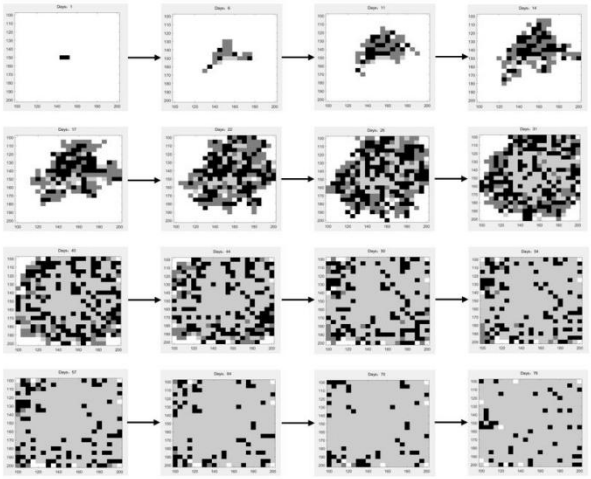

Figure 19: High temperature conditions in the Canadian region

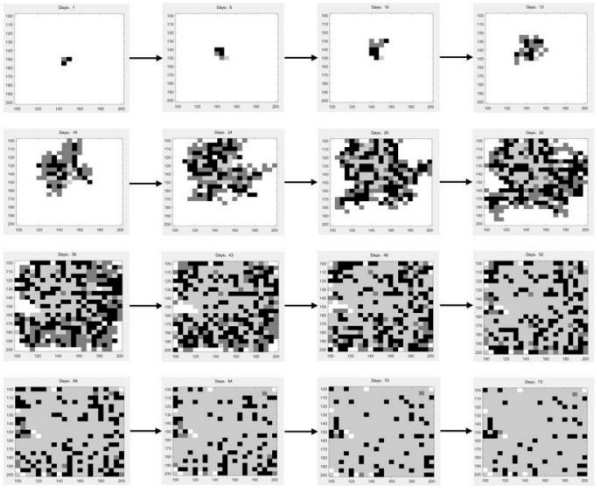

Figure 20: Drought conditions in the Canadian region

The above figure simulates the high temperature and drought in some regions of Canada, and it can be seen that with the occurrence of La Niña event, the high temperature and drought in Canada gradually appear, which in turn brings great impact on its agricultural production. The sensitivity analysis of the extreme weather-induced high temperature and drought impact model based on two-layer TOPSIS is conducted by Cellular Automata, and the reasonableness and robustness of the model establishment are illustrated by simulating the propagation process of high temperature and drought under La Niña event.

5.2 Model Checking

For the model established in the full paper, the sensitivity of the La Niña extreme climate impact model is tested by perturbing the influencing factor index of the model. In this paper, the influencing factor of greenhouse gas concentration is selected to explore the accuracy of the model, and the robustness of the model is reflected by predicting its TLNI value.

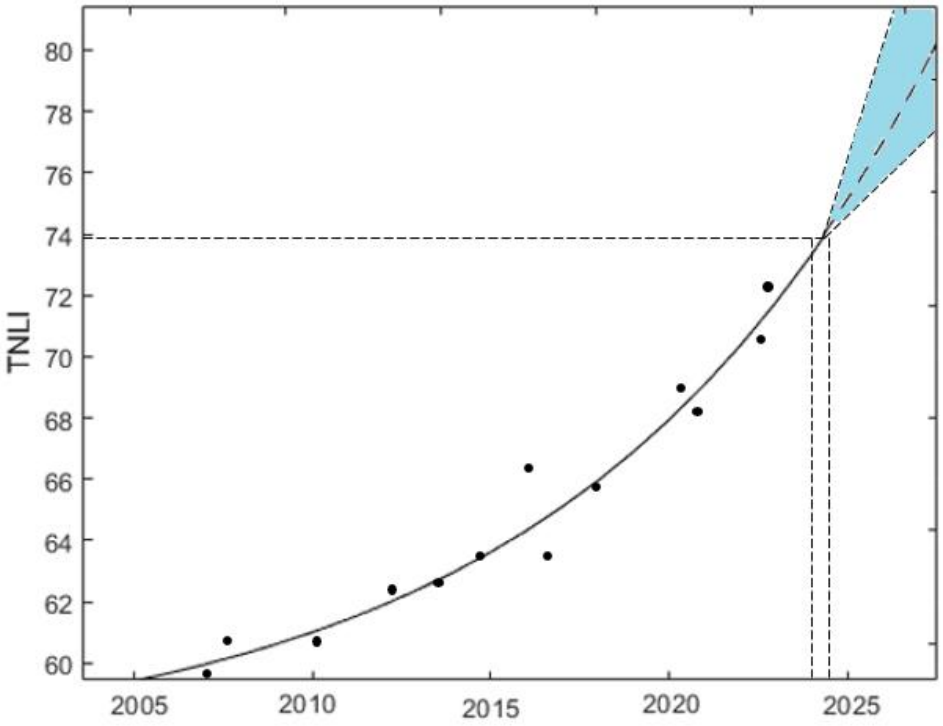

Figure 21: Model Sensitivity Analysis Chart

The above graph shows that the TLNI indicator of the model appears above the blue area in the case of controlling greenhouse gases, while the EPI indicator of the model appears below the blue area in the case of not controlling greenhouse gases. The 95% confidence interval of the model is less than 0.05, which indicates the accuracy of the prediction results. The above figure also shows that the La Niña extreme climate model can reflect the extreme climate related changes very well. Therefore, it can be concluded that the assessment model developed in this paper is robust and can be used to solve the problems presented in the topic and even extended to real-life problems.

6. Model Evaluation

6.1 Strengths

- Cellular automata can simulate complex natural phenomena, is the combination of spatial interaction and temporal causality, and has strong ability to simulate complex spatiotemporal evolution process.
- The extreme climate impact assessment model can well analyze the impact of high temperature, drought and flood disasters caused by La Niña event, and propose measures according to relevant indicators.
- The double-layer Hopfield neural network has a real-time dynamic feedback output, which makes the network more realistic in reflecting the continuity of data changes in problems such as training dynamic time models of data.

- The double-layer TOPSIS comprehensive evaluation method makes full use of the raw data information, and the results can accurately reflect the gaps between different evaluation schemes. The advantages of the method is that the calculation is simple.

6.2 Weaknesses

- The extreme climate impact assessment model does not fully consider economic and political factors, so it is necessary to include the impact of some human factors such as economic and political factors.
- The interpret ability of the two-layer feedback neural network model is poor, and the model cannot work when the data is not sufficient.
- The data of each index required by the double-layer TOPSIS comprehensive evaluation method, corresponding to the selection of quantitative indicators will be difficult, and there must be more than two research objects to be used.

6.3 Conclusion

This paper analyzes the La Niña incident and makes a summary here. The two-layer Hopfield neural network predicts the possibility of La Niña event. It is found that the probability of occurrence in China, Australia, Indonesia, Brazil, India, Canada and the United States in the next five years is less than 0.2, and the probability of occurrence after 2025 is less than 0.1. Therefore, it is reasonable to say that people have realized the impact of extreme climate and started to take a series of actions to protect the earth and the environment, The sensitivity of the prediction results was analyzed, and the error was within 6.91%. It is reasonable to believe the accuracy of the prediction results. Then this paper establishes an extreme climate impact model based on double TOPSIS for the impact of high temperature and drought to assess the losses caused by high temperature and drought. Through the model, the values of dryness index, humidity index, Demarten drought index, heat wave index and other indicators are calculated, which are 5.1, 5.7, 4.9, 4.5 and 4.9 respectively. To solve the third problem, this paper establishes the F-TLN model based on the U-Net High Grade Two water body extraction assistance to assess the disaster losses caused by floods. The U-Net network uses 300 Epochs for pre training, and inputs the images of Hubei Province into the U-Net network for water body extraction. The indicators obtained from U-Net network are combined with the corresponding indicators of DLFI to analyze China. The values of flood disaster related indicators are 6.1, 7.7, 6.9, 5.5, 6.9 and 7.1.

7. References

[1] Kun Yi Yang,Chun Xia An. Stability analysis of the three-dimensional environment pollution dynamical system[C]//.

[2] Mei Kai,Tan Meifang,Yang Zhihui,Shi Shaoyue. Modeling of Feature Selection Based on Random Forest Algorithm and Pearson Correlation Coefficient[J]. Journal of Physics: Conference Series,2022,2219(1).

[3] Najm Omar,El-Hassan Hilal,El-Dieb Amr. Optimization of alkali-activated ladle slag composites mix design using taguchi-based TOPSIS method[J]. Construction and Building Materials,2022,327.

[4] Yu Wangwang,Liu Xinwang. Behavioral Risky Multiple Attribute Decision Making with Interval Type-2 Fuzzy Ranking Method and TOPSIS Method[J]. International Journal of Information Technology & Decision Making,2022,21(02).

[5] Šverko Zoran,Vrankić Miroslav,Vlahinić Saša,Rogelj Peter. Complex Pearson Correlation Coefficient for EEG Connectivity Analysis[J]. Sensors,2022,22(4).

[6] Zhang Huiyuan,Wei Guiwu,Wei Cun. TOPSIS method for spherical fuzzy MAGDM based on cumulative prospect theory and combined weights and its application to residential location[J]. Journal of Intelligent & Fuzzy Systems,2022,42(3).

[7] Kustiyahningsih Y,Rahmanita E,Anamisa D. R.. Hybrid FAHP and TOPSIS to determine recommendation for improving SMEs facing Covid-19 pandemic[J]. Journal of Physics: Conference Series,2022,2193(1).

[8] Keddous Fekhr Eddine,Nakib Amir. Optimal CNN–Hopfield Network for Pattern Recognition Based on a Genetic Algorithm †[J]. Algorithms,2021,15(1).

[9] Xin Huang,Lin Qiu. Assessment of Soil Environment Pollution Based on Fuzzy Pattern Recognition Model[J]. Nature Environment and Pollution Technology,2021,20(4).

[10] Vadim Azarov,Vadim Kutenev. Modern Invisible Hazard of Urban Air Environment Pollution When Operating Vehicles That Causes Large Economic Damage[J]. American Journal of Artificial Intelligence,2021,5(2).

[11] Popescu Catalin,Gheorghiu Sorin Alexandru. Economic Analysis and Generic Algorithm for Optimizing the Investments Decision-Making Process in Oil Field Development[J]. Energies,2021,14(19).

[12] Li Shi Jie,Sun Bin,Hou Ding Xia,Jin Wei Jian,Ji Yun. Does Industrial Agglomeration or Foreign Direct Investment Matter for Environment Pollution of Public Health? Evidence From China [J]. Frontiers in Public Health,2021,9.

[13] Ranta Ovidiu,Marian Ovidiu,Muntean Mircea Valentin,Molnar Adrian,Ghețe Alexandru Bogdan,Crișan Valentin,Stănilă Sorin,Rittner Tibor. Quality Analysis of Some Spray Parameters When Performing Treatments in Vineyards in Order to Reduce Environment Pollution[J]. Sustainability,2021,13(14).

[14] Merikh-Nejadasl Atieh,El Makrini Ilias,Van De Perre Greet,Verstraten Tom,Vanderborght Bram. A generic algorithm for computing optimal ergonomic postures during working in an industrial environment[J]. International Journal of

Industrial Ergonomics,2021,84.
[15] Mai Weiming,Lee Raymond S. T.. An Application of the Associate Hopfield Network for Pattern Matching in Chart Analysis[J]. Applied Sciences,2021,11(9).
[16] Xu Xitong,Chen Shengbo. Single Neuronal Dynamical System in Self-Feedbacked Hopfield Networks and Its Application in Image Encryption[J]. Entropy,2021,23(4).
[17] Stefano Fazzino,Riccardo Caponetto,Luca Patanè. A new model of Hopfield network with fractional-order neurons for parameter estimation[J]. Nonlinear Dynamics,2021(prepublish).
[18] Kandali Khalid,Bennis Lamyae,Bennis Hamid. A New Hybrid Routing Protocol Using a Modified K-Means Clustering Algorithm and Continuous Hopfield Network for VANET[J]. IEEE ACCESS,2021,9.
[19] S. Malligarjunan, M. Chandrasekaran, G.B. Bhaskar. Investigation on the effect of support structure space in determining optimal part orientation using a generic algorithm[J]. International Journal of Manufacturing Technology and Management,2021,35(6).
[20] Alfulayyih Yasir M.,Li Peiwen,Gwesha Ammar Omar. A Generic Algorithm for Planning the Year-Round Solar Energy Harvest/Storage to Supply Solar-Based Stable Power[J]. Journal of Solar Energy Engineering,2020,142(4).
[21] Alexander Rybalov. A generic algorithm for the word problem in semigroups and groups[J]. Journal of Physics Conference Series,2020,1546(1).
[22] Wang Yibo,Hu Qinghe. Research and Application of Fast and Elitist Non-Dominated Sorting Generic Algorithm in Coal Blending Optimization[J]. IOP Conference Series: Earth and Environmental Science,2019,384.
[23] Silva, Karita Almeida,de Souza Rolim, Glauco,de Oliveira Aparecido, Lucas Eduardo. Forecasting El Niño and La Niña events using decision tree classifier[J]. Theoretical and Applied Climatology,2022(prepublish).
[24] Cao Ting-Wei,Zheng Fei,Fang Xiang-Hui. Key Processes on Triggering the Moderate 2020/21 La Niña Event as Depicted by the Clustering Approach[J]. Frontiers in Earth Science,2022.
[25] van Eyden, Renee,Gupta, Rangan,Nel, Jacobus,Bouri, Elie. Rare disaster risks and volatility of the term-structure of US Treasury Securities: The role of El Niño and La Niña events[J]. Theoretical and Applied Climatology,2022(prepublish).
[26] Li, Jing,Mu, Lin,Zhong, Linhao. Frequent central Pacific La Niña events may accelerate Arctic warming since the 1980s[J]. Acta Oceanologica Sinica,2022,40(11).
[27] Riza Muhammad,Putri Mutiara R,Mandang Idris. Comparison of volume transport in the Halmahera Sea between La Niña 2011 and El Nino 2015 events based on numerical model[J]. IOP Conference Series: Earth and Environmental Science,2020,618(1).
[28] Atmosphere Research; Studies from Beijing Normal University Yield New Data on Atmosphere Research (Drought-Modulated Boreal Forest Fire Occurrence and Linkage with La Niña Events in Altai Mountains, Northwest China)[J]. Science Letter,2020.